Proceedings of 2023 IEEE
International Conference on Mechatronics and Automation
August 6 - 9, Harbin, Heilongjiang, China

Preliminary Exploration of Haptic-enabled Therapist-in-the-Loop Telerehabilitation System for Exoskeleton-assisted Upper Limb Training

He Li[1], Shuxiang Guo[1,2], Hanze Wang[1], Dongdong Bu[1]*

1.The Key Laboratory of Convergence Biomedical Engineering System and Healthcare Technology, The Ministry of Industry and Information Technology, Beijing Institute of Technology, Beijing 100081, China

2. The Department of Electronic and Electrical Engineering, Southern University of Science and Technology, Shenzhen, Guangdong 518055, China

** Corresponding author: guoshuxiang@bit.edu.cn*

***Abstract* - Faced with the increase in upper limb hemiplegia caused by stroke, robotic exoskeleton-assisted home-based telerehabilitation has attracted increasing attention in recent years. Telerehabilitation is a viable alternative to traditional face-to-face rehabilitation training, which has many advantages. In this paper, a preliminary therapist-in-the-loop haptic-enable telerehabilitation system for upper limb training is presented. In the telerehabilitation system, a high-definition haptic device manipulated by the operator (served as the therapist) is the master side, and the designed upper limb rehabilitation exoskeleton worn by the subject (served as the stroke patient) is the slave side. The master-slave side realizes the operation and force data transmission through TCP/IP communication protocol. Through experiments, the angle error and time delay are analyzed, which proves the usability of the constructed system and lays the foundation for the subsequent research.**

Index Terms - Upper limb telerehabilitation, exoskeleton robot, therapist-in-the-loop, master-slave system, haptic feedback.

I. INTRODUCTION

Hemiparesis of upper limb is a common sequela of stroke [1], which occurs in about 85% of patients in the early stage. Particularly, rehabilitation training is most effective in the first 3 months after the onset of stroke [2]. Therefore, rehabilitation training in the early stage of stroke is vital. But the upper limb rehabilitation training for hemiparesis patients requires long-term training under the guidance of professionals [3], which is not easy. Long-term professional rehabilitation training requires families to bear high costs [4], and at the same time puts forward further requirements for the workload of physiotherapists. The inability to support high costs and the lack of medical resources eventually lead to the interruption of training, thus unable to ensure timely and effective treatment, resulting in missing the optimal recovery period.

During recent years, the robot-assisted device has been applied for improving the functional movements of hemiplegic patients[5]-[8], which can provide a quantitative and objective evaluation for the rehabilitation process [9][10]. Furthermore, robot-assisted training can improve the participation motivation of hemiparesis patients than traditional training way, and the portable upper limb rehabilitation robot further meets the requirements of home rehabilitation. During recent years, different upper limb rehabilitation exoskeleton systems are proposed. Liu et al. [11] showed a bilateral rehabilitation system to realize real-time stiffness adjustment through sEMG-based stiffness control. Yang et al. [12] proposed a sEMG-based bilateral training system, offline and online experiments were designed to verify the rehabilitation training system. Xiao et al. [13] presented a cable-driven upper limb exoskeleton with seven degrees of freedom, which is compact, lightweight, and comfortable for post-stroke patients.

Traditional robot-assisted training lacks the expert guidance of therapists in real-time. The therapist plays an irreplaceable role in adapting rehabilitation strategies and intensity to meet the specific need for each patient, while the application of robots has the potential to assist the therapist and facilitate the process of rehabilitation assessment. Therefore, further tele-rehabilitation attracts more and more attention. Popescu et al. [14] presented ongoing research activities for developing and functional testing of an upper limb rehabilitation robotic system. Chen et al. [15] presented a novel telerehabilitation system based on a bilateral upper limb exoskeleton robot, which is aimed at the classification of discrete movements. But the upper limb rehabilitation should focus more on continuous motion rather than discrete motion. Atashzar et al. [16] proposed a new framework for neural-network-based supervised training of intensity and strategy for upper-limb haptics-enabled robotic neurorehabilitation systems for poststroke motor disabilities. However, the high cost of the robot in slave side makes it unsuitable for home-based rehabilitation.

In this paper, a therapist-in-the-loop tele-rehabilitation system for upper limb training is built, in which the therapist in the hospital guides the rehabilitation training of the stroke patient at home. The master side adopts a haptic device, and the slave side adopts an upper limb rehabilitation exoskeleton to drive upper limb movement. The structure of the rest of this paper is organized as follows. Section II describes the involved methods one by one, which mainly include the overview of the tele-rehabilitation system, the haptic device, the design and control of the exoskeleton, the User Datagram Protocol (UDP) communication in Local Area Network (LAN), and the force sensor. The experiments and results are shown in Section III. Finally, section IV presents the conclusion.

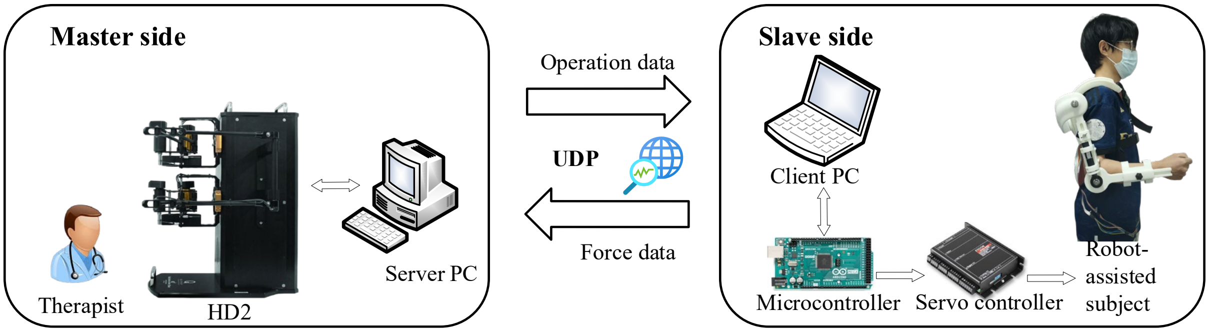

Fig. 1 The Overall diagram of the therapist-in-the-loop tele-rehabilitation system in this study

II. METHODS

In our therapist-in-the-loop tele-rehabilitation system (as shown in Fig.1), the master side with a haptic device is for therapists, and the slave side with an upper limb rehabilitation exoskeleton is for patients. A TCP/IP communication is used to transmit the operation data and force feedback between the master side and the slave side.

A. Haptic Device

The Quanser High Definition Haptic Device [17] is a high-fidelity haptic interface for advanced research in haptics and robotics. The HD2 enables researchers to interact with virtual or remote environments using programmable force feedback and gives them uniquely large workspace and very low intervening dynamics. It is also highly back-drivable with negligible inertia and friction. The HD2 system includes the following main components: the haptic robot, the E-Stop button, the data acquisition card (DAQ), the DAQ to HD2 interface box, and the input pedals. The components of the HD2 are shown in Fig.2. How these and other components interact with each other is illustrated in Fig.3. This also shows how the system can be controlled through a client-server paradigm using various client applications. A user push pedal (as shown in Fig.2b) is provided with the device as a digital input for switching applications. The E-Stop (as shown in Fig.2c) must be connected to the HD2 for proper operation. The E-Stop button locks in the disabled position when pressed to guarantee the patient's safety. To release the E-Stop, twist the red button clockwise.

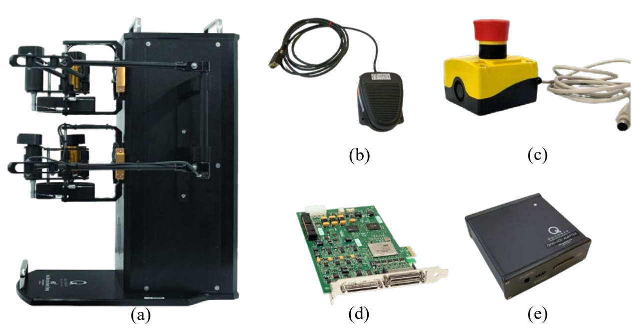

Fig. 2 HD2 components (a) HD2 (b) Input pedal (c) E-Stop push button (d) QPIDe DAQ device (e) QPIDe to HD2 interface box

The HD2 system is run in MATLAB/Simulink using the QuaRC real-time environment, which is provided by the industrial partner of this work Quanser (Markham, ON, Canada). The underlying language environment of QuaRC is Visual Studio. QuaRC is fully compatible with MATLAB and implements hardware-in-the-loop, and its own module library is embedded in the Simulink module library. Meanwhile, QuaRC supports a variety of communication protocols (TCP/IP, UDP, serial port, etc.) and is compatible with third-party devices (Kinect, Logitech camera, etc.).

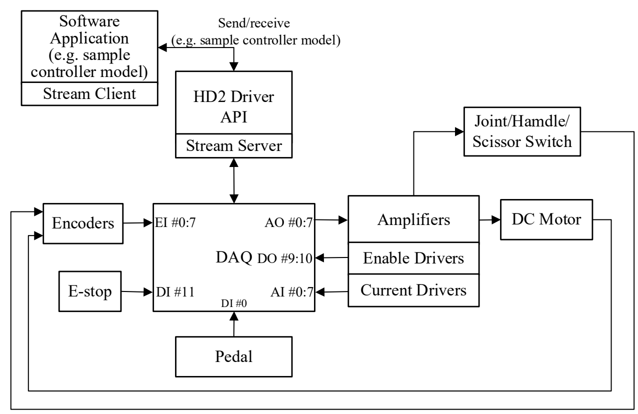

Fig. 3 HD2 component interaction

B. Exoskeleton Design and Control

The overview of the gear-driven powered upper limb exoskeleton device (GP-ULED) is shown in Fig.4. It has 2 passive shoulder degrees of freedom (DoFs) which are shoulder adduction/abduction and shoulder flexion/extension, and 1 active elbow DoF which is elbow flexion/extension (passive DoF means the rotation due to human movements, active DoF means rotation due to the gear-driven mechanism). The length of the upper arm of the exoskeleton and the position of the forearm underframe can be adjusted. To reduce the structural weight and cost while considering accuracy, the main exoskeletal frames are 3D printed in curable resin, which is lightweight and allows for small physical configurations and high versatility to suit different users. The total weight of GP-ULED is only 1.35 kg which is shared by 2 fabric straps (as shown in Fig.4b, one around the loin, and one shoulder harness) to the torso.

A gear-driven elbow exoskeleton (Fig.4a) powered by a brushless motor (EC 22, 40, Maxon, Switzerland) is used as the slave side. The brushless motor which has a built-in Hall sensor couples with a gearbox (Maxon Planetary Gearhead GP 22 HP) and a quadrature optical encoder (MR M-512) which is used to control the rotation angle of the elbow joint with the help of gear. Compared with single-channel encoders, quadrature encoders can provide higher resolution and have strong immunity to interference. The brushless motor is placed along the upper arm which reduces the forearm burden and obstacles. And the motor is controlled by a specialized servo controller (ESCON 50/5, Maxon) with four-quadrant Pulse-Width Modulation (PWM). The bevel gears are made of 45 steel, and the ratio between the two bevel gears is 1:2. In addition, the backlash between the two gears can be shortened by adjusting their position with the help of the oblong fixation base of the motor.

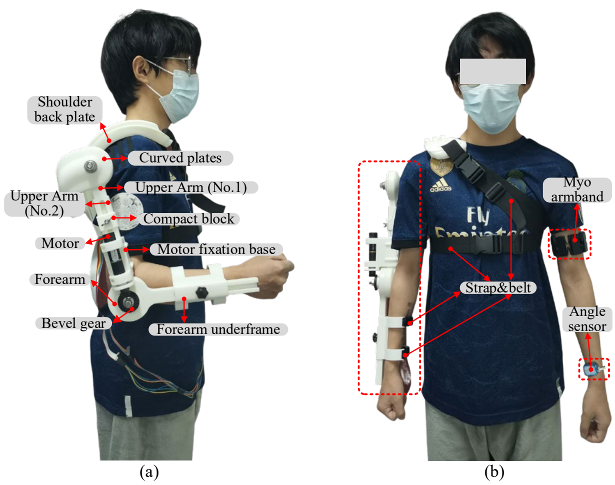

Fig. 4 The upper limb exoskeleton device. (a) lateral view (b) front view.

The control of the exoskeleton and data logging are executed through a microcontroller (Arduino Mega 2560), which collects the HD2 angle data transmitted to the slave PC. The USB connection creates a virtual COM Port on the PC for UART communication link between Arduino and the Simulink of slave PC. The ESCON servo controller enables Arduino to directly control the motor using 3-pin interface: PWM, Clockwise (CW), and Counter Clockwise (CCW). The motor speed is controlled by adjusting PWM duty cycle, and the range of the PWM duty cycle is from 10% to 90%. The PWM input frequency range of the ESCON is from 10Hz to 5kHz, a good compromise in practice offering fast reaction and precise duty cycle measurement is to use 1 kHz which needs 1ms for signal processing, so 1kHZ is selected as the PWM output frequency of Arduino. The real-time control is based on an outer position and an inner velocity loop. In the drive control of the servo driver to the motor, the Hall sensor inside the servo motor feeds the information to the servo driver, and the servo driver uses feedback information to adjust to achieve the speed closed-loop control of the servo motor. In outer position loop of bilateral rehabilitation, the control system uses the deviation of the intact side angles and the exoskeleton motor angle to carry out proportional-integral-differential (PID) closed-loop control, in which the duty cycle of PWM is adjusted according to the position error, so as to control the motor speed. The formula of PID is shown in (1). To count encoder pulses using hardware interrupts to feed back the actual position of the motor to Arduino, encoder channel A and B should be connected to the Arduino interrupt pin. Here, 1x count is adopted for encoder pulses. The reason why the 1x count is chosen instead of the 4x count is to avoid program disorder caused by too many interruptions entered because the encoder itself has a higher resolution (pulses per revolution=512) and the planetary gear reduction box has a higher reduction ratio (reduction ratio=270). Fig.5 presents the overall design of the embedded system of GP-ULED.

$$U(t) = K_p e(t) + K_t \int e(t)dt + K_d \frac{d}{dt} e(t) \quad (1)$$

Where $U(t)$ represents the PWM output, $e(t)$ represents the error of the intact side angle and the exoskeleton motor angle, K_p, K_t, and Kd is the proportional coefficient, integral coefficient, and differential coefficient, respectively.

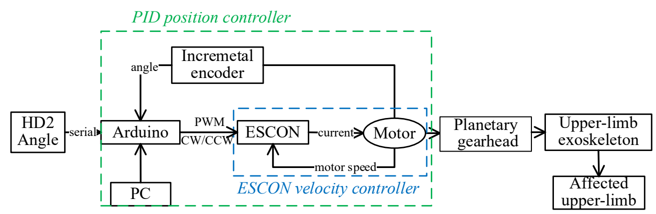

Fig. 5 Overall design of the embedded system.

C. UDP LAN communication

A LAN is a connected environment spanning one or more buildings – typically in a one-kilometer radius – that links computing devices within close proximity of each other by using ethernet and Wi-Fi technology. Compared to Wide Area Network (WAN), LAN is simpler and more suitable for our research which is just in the early stage. Therefore, the LAN between the master and slave computer is set up.

Based on LAN, the network protocol is further considered. TCP/IP has two representative transport layer protocols, namely TCP and UDP. Compared with TCP, UDP is an unreliable and connectionless protocol. That is to say, there is no need to establish a connection prior to data transfer. But the UDP helps to establish low-latency and loss-tolerating connections over the network. Considering the real-time requirement of tele-rehabilitation system, UDP is selected as the communication mode. Based on the above consideration, the UDP communication in LAN is built in this study.

The HD2 system supports a variety of communication protocols, including UDP. The “Receive UDP” module is used in the master side, and the IP address is set according to the IP address of the master PC, as shown in Fig.6a. The “Send UDP” module is used in the slave side, the IP address is set according to the IP address of the slave PC, as shown in Fig.6b.

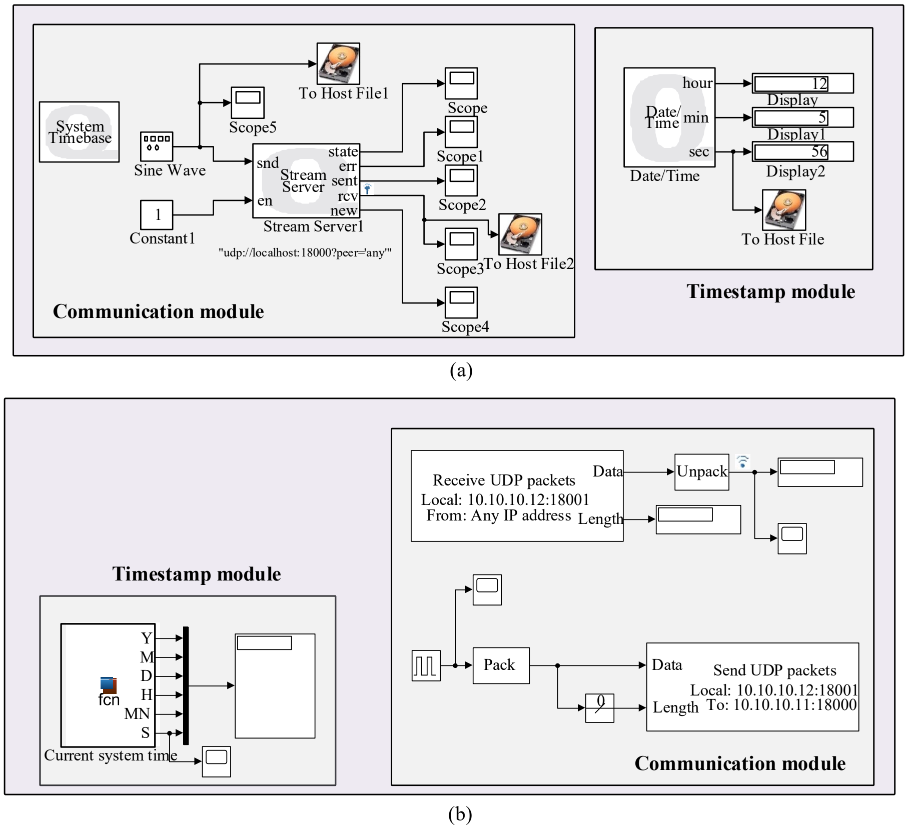

Fig. 6 Communication module (a) master side (b) slave side.

Since the system time of the master and slave computer may be biased, it is necessary to synchronize the time, here the time is synchronized through the Network Time Protocol (NTP) protocol which is an application layer protocol within the TCP/IP protocol family. Based on the LAN adopted in this study, it can typically provide an accuracy of less than a millisecond. To test the communication delay of the master and slave computer, the system time needs to be recorded with the help of a timestamp. The slave computer obtains its system time with the help of the "*MATLAB function*" module, as shown in Fig.6a. The host computer obtains its system time with the "*Data/time*" module in QuaRC [18], as shown in Fig.6b.

D. Force Sensor

Force Sensing Resistors (FSR) are a polymer thick film device which exhibits a decrease in resistance with an increase in the force applied to the active surface. The FSR 402 [19] is a kind of FSR, which also will vary its resistance depending on how much pressure is being applied to the sensing area. The harder the force, the lower the resistance. Only one side of the sensor is pressure sensitive and the same side must be used to apply force. This sensor is put in the circuit like other resistors to get the output. When no pressure is being applied to the FSR 402, its resistance will be maximum or infinitive. The pressure sensor can be converted into a voltage signal that can be recognized by the microcontroller, and the simplest way to read the FSR 402 is to combine it with a static resistor to form a voltage divider. However, the resistor division method has disadvantages such as poor linearity and poor adaptability of different types of sensors, an op amp-based signal conversion module is adopted in this study. The module has high output linearity, adjustable magnification and high measurement accuracy. The output range is 0-3.3V, compatible with 5V and 3.3V control systems. Fig.7 shows the connection diagram between FSR402 and Arduino. The sensing area of FSR402 is around with 16mm diameter. The formula between the output voltage and the applied pressure is as shown in (2).

$$U_0 = \frac{3.2}{F_{max}} \times F + 0.1 \tag{2}$$

Where U_0 is the output voltage of the conversion module, F is the pressure value.

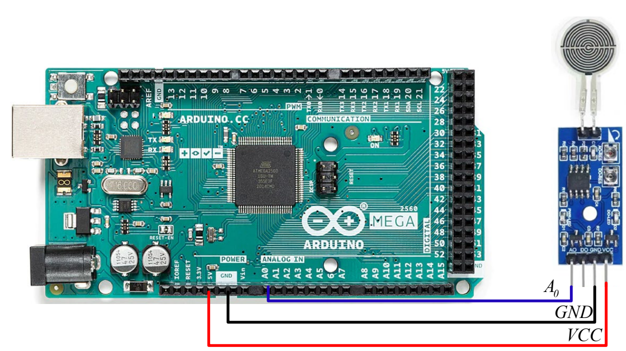

Fig.7. Connection diagram between FSR402 and Arduino.

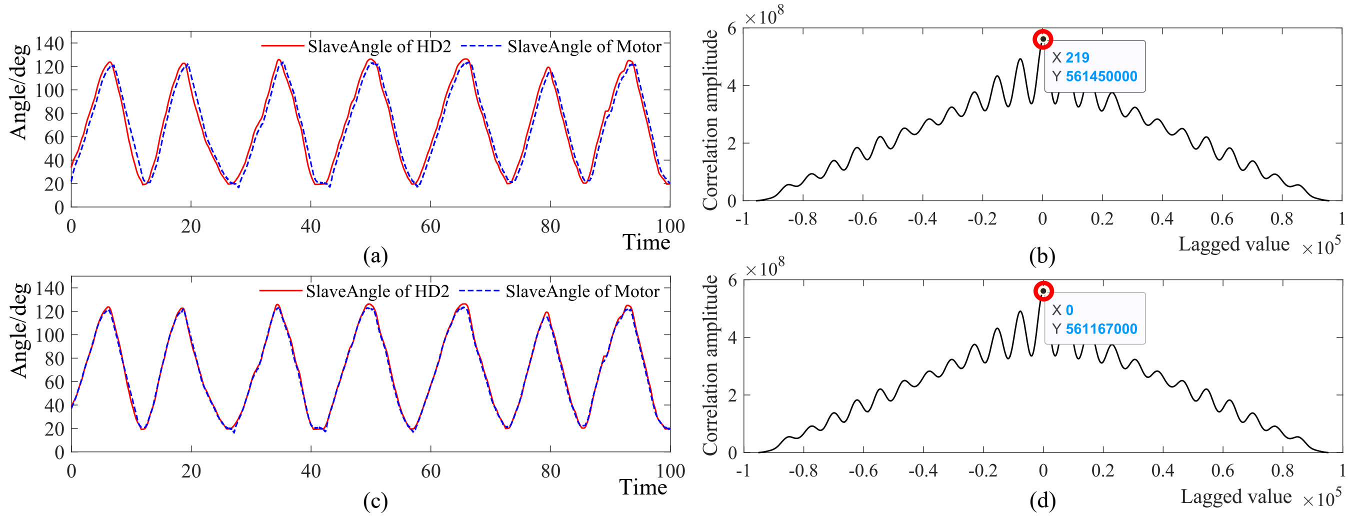

Fig 10. The angles of HD2 and exoskeleton motor in the slave side. (a) angle with time lag (b) phase difference between the angle of HD2 and exoskeleton motor (c) angle without time lag (d) phase difference between the angle of HD2 and exoskeleton motor after time lag elimination.

III. EXPERIMENTS AND RESULTS

To verify the effectiveness of the proposed telerehabilitation system, a master-slave control experiment is conducted. The experimental setup consists of one HD2 haptic device acting as the therapist's robot, and one upper limb rehabilitation exoskeleton serving as the patient's robot. The UDP is used to transmit data between the master robots and the slave robot. All controllers and the communication between the robots were implemented using the QuaRC Real-Time system at a sampling frequency of 0.5 kHz. Fig.8 shows the experimental setup.

The experiment is performed in two DOFs, along the sagittal-transverse plane. HD2 is along the transverse plane, and the exoskeleton is along the sagittal plane. In the experiment, two operators are asked to simulate behaviors of a typical therapist and a typical patient to evaluate the proposed system. The operators are familiar with the setup. The subject on the master side operated the handle of HD2, then the angle information is sent to the slave side to control the exoskeleton device. A force sensor (FSR402) is used to record the force produced in the slave side, and then the value is transferred to the master side, then the operator can feel the force through the HD2 robot.

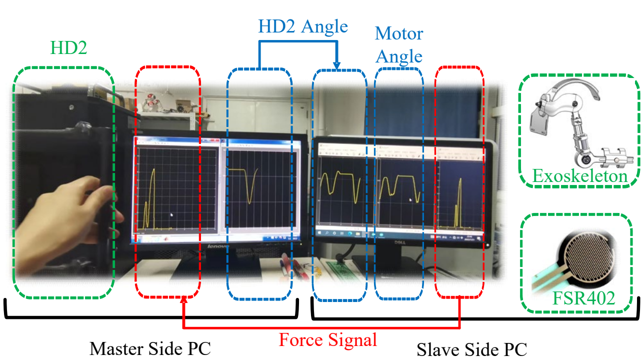

Fig. 8 The experimental setup

A. The communication delay between master and slave computer

In the experiment for the master-slave computer communication delay test, the master computer sends a sine wave to the slave computer, and the slave computer sends a pulse signal to the master computer. In the many experiments for the communication delay test performed in this study, the delay of each experiment is controlled within 10ms. Fig. 9 shows the results of one of the experiments. As can be seen from this figure, the delay in sending signals from the master PC to the slave PC is 12 sample points, and the delay in sending signals from the slave PC to the master PC is 20 sample points. Since the sampling frequency is 1kHz, the delay is 12ms and 20ms, respectively.

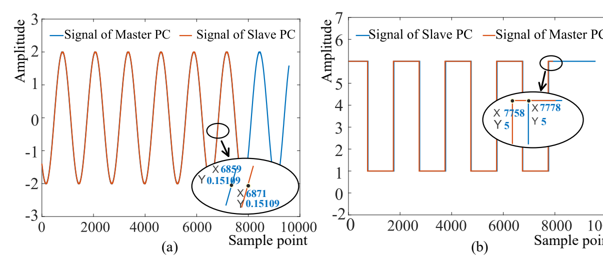

Fig. 9 The experimental result of communication delay (a) a sine wave signal sent from master to slave side (b) a pulse wave signal sent from slave to master side

B. Master-slave position tracking

Fig.10 records the angles of HD2 and the exoskeleton motor in the slave side, and the time delay between the two kinds of angles. Fig.10a shows the angular amplitude between the HD2 angle and motor angle in the slave side. The mutual correlation (Matlab "*xcorr*" function) is adopted to calculate the time difference. Fig.10b is the calculation result, with a time difference of 219 sample points. Due to that the sampling frequency is 0.5kHz, so according to (3), the time difference is 438ms. Fig.10c shows the angular amplitude between the HD2 angle and motor angle in the slave side after time lag elimination. Fig.10d is the calculation result after time lag elimination, there is no delay at this time, so the calculation result is 0.

$$T_{diff} = \frac{1}{F_s} * S \tag{3}$$

Where T_{diff} is the calculation result of the time difference, F_s is the sampling frequency of the QuaRC Real-Time system, S is the sample point number of time difference.

To quantitatively evaluate the angle error between HD2 and the exoskeleton motor in the slave side, the evaluation index of Mean Absolute Error (MAE) [20] is adopted, as recorded in Table I. MAE represents the average of the absolute error between the expected value and the observed value, as shown in (4). Table I shows that the MAE before time lag elimination is 6.2657, and the MAE after time lag elimination is 1.4170. which indicates that the angle error is largely due to the delay in the control of the exoskeleton.

$$MAE = \frac{1}{N} \sum_{i=1}^{N} | y_i - x_i | \tag{4}$$

Where x_i represents the angle of HD2 at *i*th data point, and y_i represents the angle of the exoskeleton at *i*th data point, and *N* is the total number of data points.

TABLE I
EVALUATION OF THE EXPERIMENTAL RESULTS

MAE	With Time Delay	6.2657
	Without Time Delay	1.4170

IV. CONCLUSION

In this study, a therapist-in-the-loop telerehabilitation system for upper limb training is proposed, in which HD2 is manipulated by the therapist in the master side and the rehabilitation exoskeleton is worn by the stroke patient in the slave side. The master side sends operation data to the slave side to control the upper limb exoskeleton to assist the upper limb movement, and the slave side sends force data to the master side so that the operator in the master side can feel the force produced in the slave side. Through the designed experiment, the feasibility of the telerehabilitation system is verified, which is the basic work for future research.

As for the following research, due to the real-time characteristics of the human-machine interface, the response time of the system should be less than 300ms. However, the time delay in this study is 438ms, which exceeded the stipulated time. Therefore, one of the key points of future research is to shorten the response time and improve the real-time performance of the system. Another research point is to combine virtual reality to increase the user's experience.

REFERENCES

[1] F. C. Ersoy, and G. Iyigun, "Boxing training in patients with stroke causes improvement of upper extremity, balance, and cognitive functions but should it be applied as virtual or real?," Topics in Stroke Rehabilitation, vol. 28, DOI 10.1080/10749357.2020.1783918, no. 2, pp. 112-126, Mar. 2021.

[2] G. Poomalai, S. Prabhakar, N. Sirala Jagadesh, "Functional Ability and Health Problems of Stroke Survivors: An Explorative Study," Cureus, vol. 15, DOI 10.7759/cureus.33375, no.1, e33375, Jan. 2023.

[3] G. Kim, S. Lim, H. Kim, B. Lee, S. Seo, K. Cho, et al., "Is robot-assisted therapy effective in upper extremity recovery in early stage stroke? -a systematic literature review," Journal of Physical Therapy Science, vol. DOI 10.1589/jpts.29.1108 29, no. 6, pp.1108-1112, Jun. 2017.

[4] J. Narayan, B. Kalita, and S. K. Dwivedy, "Development of Robot-Based Upper Limb Devices for Rehabilitation Purposes: a Systematic Review," Augmented Human Research, vol. 6, DOI 10.1007/s41133-020-00043-x, no. 1, pp. 1-33, Jan. 2021.

[5] R. Gopura, D. Bandara, K. Kiguchi, and G. K. Mann, "Developments in hardware systems of active upper-limb exoskeleton robots: A review," Robotics and Autonomous Systems, vol. 75, pp. 203-220, 2016.

[6] M. Gandolfi, N. Valè, E. K. Dimitrova, S. Mazzoleni, E. Battini, M. Filippetti, et al., "Effectiveness of Robot-Assisted Upper Limb Training on Spasticity, Function and Muscle Activity in Chronic Stroke Patients Treated With Botulinum Toxin: A Randomized Single-Blinded Controlled Trial," Frontiers in Neurology, https://doi.org/10.3389/fneur.2019.00041, 2019.

[7] C. Lauretti, F. Cordella, E. Guglielmelli, and L. Zollo, "Learning by Demonstration for planning activities of daily living in rehabilitation and assistive robotics," IEEE Robotics and Automation Letters, vol. 2, no. 2, pp. 1375-1382, 2017.

[8] N. Smania, N. Valè, E. Dimitrova, S. Mazzoleni, M. Filippetti, C. Depaoli, et al., "Effects of high-intensity robot-assisted training in hand function recovery and adl independence in individuals with multiple sclerosis: A randomized controlled single-blinded trial," Gait & Posture, vol. 57, p. 16, 2017.

[9] A. Cerasa, L. Pignolo, V. Gramigna, S. Serra, G. Olivadese, F. Rocca, et al., "Exoskeleton-Robot Assisted Therapy in Stroke Patients: A Lesion Mapping Study," Front Neuroinform, vol. 17, DOI 10.3389/fninf.2018.00044, no. 12, 44, Jul. 2018

[10] S. Inoue, Y. Otaka, M. Kumagai, M. Sugasawa, N. Mori, K. Kondo, "Effects of Balance Exercise Assist Robot training for patients with hemiparetic stroke: a randomized controlled trial," Journal of NeuroEngineering and Rehabilitation, vol. 19, DOI: 10.1186/s12984-022-00989-6, no.1, 12, Jan. 2022.

[11] Y. Liu, S. Guo, Z. Yang, H. Hirata and T. Tamiya, "A Home-Based Bilateral Rehabilitation System With sEMG-based Real-Time Variable Stiffness," IEEE Journal of Biomedical and Health Informatics, vol. 25, DOI 10.1109/JBHI.2020.3027303, no. 5, pp. 1529-1541, May. 2021.

[12] Z. Yang, S. Guo, Y. Liu, Hi. Hirata and T. Tamiya, "An intention-based online bilateral training system for upper limb motor rehabilitation," Microsystem Technologies, vol. 27, DOI 10.1007/s00542-020-04939-x, 211–222, Jun. 2021.

[13] F. Xiao, Y. Gao, Y. Wang, Y. Zhu and J. Zhao, "Design and evaluation of a 7-DOF cable-driven upper limb exoskeleton," Journal of Mechanical Science and Technology, vol. 32, DOI: 10.1007/s12206-018-0136-y, 855–864, Feb. 2018.

[14] D. Popescu, H. Roibu, C. Copilusi, L. Rusu, T. Avramescu, M. Zavaleanu et al., "Functional Testing Procedures and Results for a Rehabilitation Robotic System," 2018 International Conference and Exposition on Electrical And Power Engineering (EPE), Iasi, Romania, DOI: 10.1109/ICEPE.2018.8559676, 512-517, Oct. 2018.

[15] J. Chen, D. Hu, W. Sun, X. Tu and J. He, "A Novel Telerehabilitation System Based on Bilateral Upper Limb Exoskeleton Robot," 2019 IEEE International Conference on Real-time Computing and Robotics (RCAR), Irkutsk, Russia, DOI: 10.1109/RCAR47638.2019.9044072, 391-396, Aug. 2019.

[16] S. Atashzar, M. Shahbazi, M. Tavakoli and R. Patel, "A Computational-Model-Based Study of Supervised Haptics-Enabled Therapist-in-the-Loop Training for Upper-Limb Poststroke Robotic Rehabilitation," IEEE/ASME Transactions on Mechatronics, vol. 23, DOI: 10.1109/TMECH.2018.2806918, no. 2, 563-574, April 2018.

[17] HD² High Definition Haptic Device, Quanser. https://www.quanser.com/products/hd2-high-definition-haptic-device/

[18] QUARC Real-Time Control Software, Quanser. https://www.quanser.com/products/quarc-real-time-control-software/

[19] FSR 402. https://www.interlinkelectronics.com/fsr-402.

[20] Stephanie Glen. "Absolute Error & Mean Absolute Error (MAE)" From StatisticsHowTo.com. https://www.statisticshowto.com/absolute-error/.